Quantum coherence enhances electron transfer rates to two equivalent electron acceptors

Brian T. Phelan‡, Jinyuan Zhang‡, Guan-Jhih Huang, Yi-Lin Wu, Mehdi Zarea, Ryan M. Young*, and Michael R. Wasielewski*

Department of Chemistry and Institute for Sustainability and Energy at Northwestern, Northwestern University, Evanston, IL 60208-3113, USA

Supporting Information Placeholder

ABSTRACT: When a molecular electron donor interacts with multiple electron acceptors, quantum coherence can enhance the electron transfer (ET) rate. Here we report photo-driven ET rates in a pair of donor-acceptor (D-A) compounds that link one anthracene (**An**) donor to one or two equivalent 1,4-benzoquinone (**BQ**) acceptors. Sub-picosecond ET from the lowest excited singlet state of **An** to two **BQs** is about 2.4 times faster than ET to one **BQ** at room temperature, but about 5 times faster at cryogenic temperatures. This factor of 2 increase results from a transition from ET to one of two acceptors at room temperature to ET to a superposition state of the two acceptors with correlated system-bath fluctuations at low temperature.

The role of quantum coherence in energy and electron transfer processes has attracted much interest in the study of both natural and artificial light-harvesting systems.[1-2] Such coherences between vibronic states of the precisely arranged chlorophylls in light-harvesting antenna complexes may contribute to the near-unity quantum yields of exciton funneling to photosynthetic reaction centers (RCs).[3-5] Although the observation of coherences in protein environments is surprising given the presumed numerous random fluctuations among the chromophores (the system) and between the system and the protein environment (the bath), related work suggests that the protein environment may actually shield the chromophores from random fluctuations, enabling coherent dynamics to persist for hundreds of femtoseconds.[6-8] These observations have also been extended to electronic energy transfer in conjugated polymers,[9] suggesting that coherence preservation via structure-correlating fluctuations may be broadly applicable.

Similar effects in electron transfer (ET) reactions within RCs and organic photovoltaic (OPV) materials have also received increased interest due to the availability of multiple acceptor sites and, in OPV materials, the role of delocalization in rapidly separating charges.[10-12] ET reactions have been modeled extensively using both semi-classical[13] and quantum mechanical[14] treatments, with the latter accounting for high frequency vibrational modes of the system. The rates of these reactions are generally described by eq 1, where k_{ET} is the ET rate

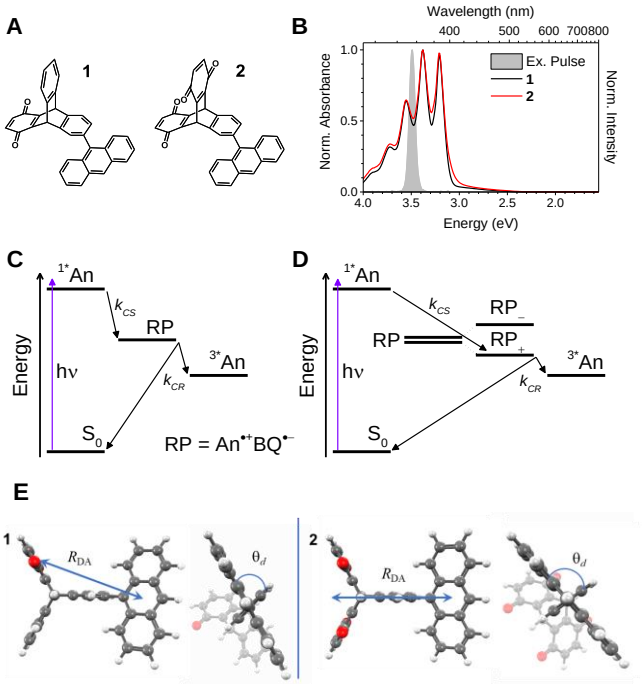

Figure 1. (A) Molecules investigated and their (B) steady-state electronic absorption spectra. Diagrams showing relevant excited state processes for (C) **1** and (D) **2**. (E) DFT-Optimized geometries for **1** and **2** showing donor-acceptor distances R_{DA} (8.39 and 7.98 Å for **1** and **2**, respectively) and dihedral angles θ_d (74° and 84° for **1** and **2**, respectively) See SI for computational details.

constant, V_{DA} is the electronic coupling matrix element between the electron donor and acceptor, and ρ is the Franck–Condon-weighted density of states:

$$k_{ET} = \frac{2\pi}{\hbar}|V_{DA}|^2\rho \quad (1)$$

Additionally, numerous theoretical studies have shown that system-bath interactions in ET can impact the site energies and donor-acceptor coupling [15] as well as destroy interference between multiple pathways.[16-17] Moreover, these studies indicate that quantum coherence can be preserved in the limit of weak system-bath coupling and low temperature.[18]

Here, we report on charge separation (CS) in a pair of donor-acceptor (D-A) compounds that link an anthracene (**An**)

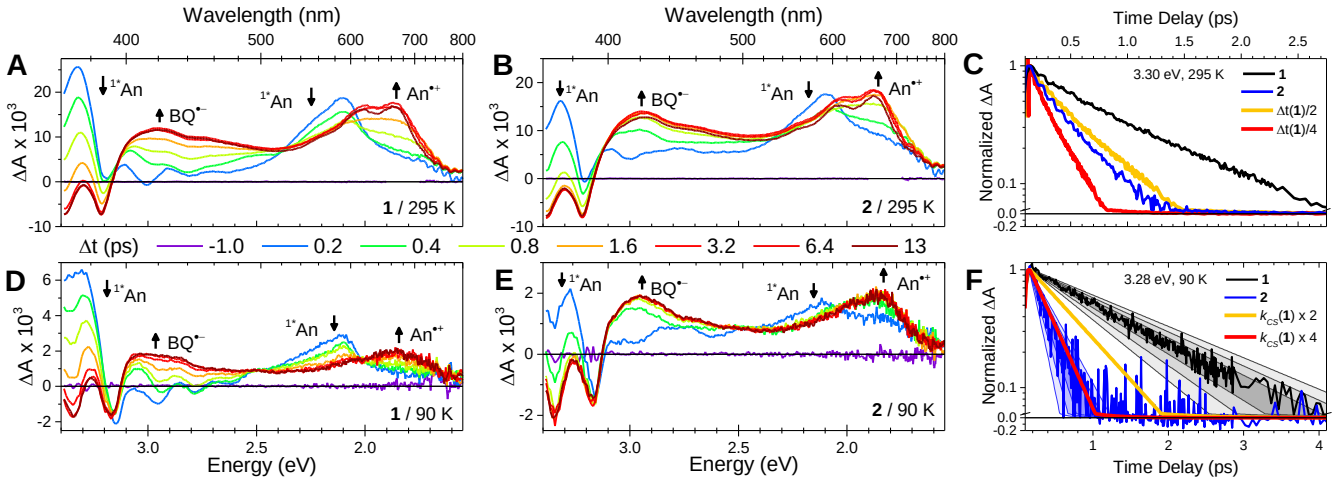

Figure 2. TA spectra of (A) **1** and (B) **2** in 1,4-dioxane at 295 K and (D) **1** and (E) **2** in glassy Me-THF at 90 K obtained with excitation at 3.49 eV (200 nJ/pulse, <50 fs). Normalized kinetic traces for **1** and **2** in (C) 1,4-dioxane, 295 K, probe energy = 3.30 eV and (F) Me-THF, 90 K, probe energy = 3.28 eV. The progressively lighter gray and blue shadings in depict the standard deviations of the average rate constant, 1σ, 2σ, and 3σ, respectively.

electron donor chromophore to one (**1**) or two (**2**) 1,4-benzoquinone (**BQ**) electron acceptors (Figure 1A). These moieties were covalently bridged by a triptycene scaffold with the **An** bonded through its 9-position to a triptycene phenyl ring. Detailed synthetic procedures and characterization are given in the Supporting Information (SI). The triptycene scaffold was chosen to provide the appropriate geometry and rigidity to incorporate two electron acceptors that are spatially indistinguishable to the electron donor.

The steady-state absorption spectra of **1** and **2** dissolved in 1,4-dioxane at 295 K are shown in Figure 1B. 1,4-Dioxane was chosen for the experiments at 295 K because its low dielectric constant (2.3) is similar to that of glassy 2-methyltetrahydrofuran (Me-THF, 2.6) at cryogenic temperatures (*vide infra*). The **An** absorption of **1** and **2** are similar to that of unsubstituted **An** (Figure S5). The low-energy shoulder in the absorption spectra of **1** and **2** likely results from an n → π^* transition, which was also observed here in a triptycene-mono(**BQ**) reference molecule (Figure S5) and elsewhere in a series of related nonconjugated arene and quinone chromophores.[19]

The ET reactions for these compounds were investigated using TA spectroscopy with a 3.49 eV (355 nm), <50 fs excitation pulse resonant with the **An** absorption in each compound and a chirped broadband probe pulse spanning 1.55–3.40 eV (800–365 nm) (see SI for instrument details). Following excitation of **1** at room temperature in 1,4-dioxane (295 K) (Figure 2A), we observed positive signals at 2.09 and 3.33 eV, corresponding to excited-state absorption (ESA) from the **An** lowest excited singlet state (^{1*}**An**) to higher-lying S_n states. Superimposed on the ESA are negative ground-state bleach (GSB) signals at 3.21 and 3.38 eV and stimulated emission (SE) at 2.81, 2.99, and 3.20 eV resulting from formation of ^{1*}**An**. These features are similar to those of **An** itself (Figure S6A) indicating that excitation at 3.49 eV predominantly populates ^{1*}**An**.[20] The SE and ESA decay rapidly to new ESA at 2.61–3.10 eV and 1.77–2.16 eV assigned to **BQ**$^{\bullet-}$ and **An**$^{\bullet+}$, respectively, showing that rapid CS occurs to yield the radical ion pair (RP) state, ^{1*}**An**–**BQ** → **An**$^{\bullet+}$–**BQ**$^{\bullet-}$ as outlined in Figure 1C.[21-22]

The TA spectra of **2** acquired at 295 K in 1,4-dioxane (Figure 2B) are similar to that of **1**, except that CS occurs more rapidly in **2**. We determined the effect of the second **BQ** acceptor on the CS rate by evaluating the ratio k_{CS}(**2**)/k_{CS}(**1**). In 1,4-dioxane at 295 K; however, CS occurs on a timescale similar to the RP relaxation process, which complicates the kinetic analysis by requiring two exponential decay functions that are highly coupled. To avoid this complication we compared kinetic traces at the ^{1*}**An** ESA for **1** and **2** by dividing the time delay Δt of the **1** kinetic trace by a factor of q = 1.0-4.5 and then evaluating the sum of the residuals-squared, $\sum \chi^2(\Delta t, q)$, between the **2** kinetic trace and the scaled **1** kinetic trace to determine which factor q best represents the CS rate enhancement afforded by the second **BQ** (Figure S9), i.e. $q \approx k_{CS}(\mathbf{2})/k_{CS}(\mathbf{1})$. The ESA feature at a single frequency (3.30 eV) was chosen for the analysis to maximize the time resolution by minimizing the effect of group velocity mismatch between the pump and the probe while still monitoring the charge separation dynamics (see SI for details). In addition, we report the rate constants at 295 K, approximated using the time delays corresponding to 1/e decay, in Table 1. This analysis indicates that at 295 K the decay rate of **2** is ~2.4 times that of **1**, consistent with prior theory.[23-25] In the incoherent limit, where thermal fluctuations of the **BQ**s or solvent disrupt the equivalency between the two sites, CS proceeds independently to either acceptor 1 (RP_1) or acceptor 2 (RP_2). Assuming $V_{DA}(RP_1) = V_{DA}(RP_2)$ in **2**, which are both equal to V_{DA} in **1**, then $k_{CS}(RP_1) = k_{CS}(RP_2) = k_{CS}$(**1**). Since the two acceptors are interacting with the donor as independent, uncorrelated sites, k_{CS}(**2**) is given statistically by $k_{CS}(\mathbf{2}) = k_{CS}(RP_1) + k_{CS}(RP_2)$, which reduces to $k_{CS}(\mathbf{2}) = 2 \times k_{CS}(\mathbf{1})$.

Table 1. Average k_{CS} reported as $(\langle\tau_{CS}\rangle \pm \sigma)^{-1}$ and ratios.

	$\langle k_{CS}\rangle$ (fs^{-1})		
	295 K	**90 K**	**5.5 K**
1	$(753 \pm 23)^{-1}$	$(1240 \pm 130)^{-1}$	$(1490 \pm 140)^{-1}$
2	$(310 \pm 10)^{-1}$	$(265 \pm 39)^{-1}$	$(297 \pm 38)^{-1}$
k_{CS}(**2**)/ k_{CS} (**1**)	2.4 ± 0.1	4.7 ± 0.8	5.0 ± 0.8

We next consider the CS dynamics for **1** and **2** in glassy Me-THF at 90 K (Figure 2D-E) and 5.5 K (Figure S7), where solvent motions are inhibited and system-bath interactions are reduced. The spectra and dynamics are similar to those for **1** and **2** in 1,4-dioxane at 295 K, except that the RP relaxation

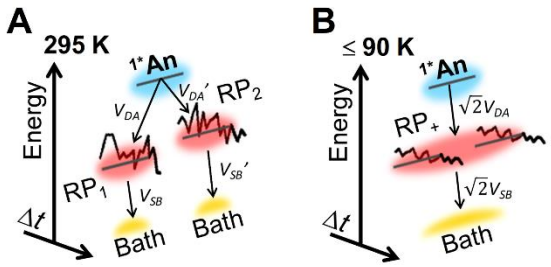

Figure 3. Schematic showing system-bath interactions involving the two acceptors (RP states) at (A) room and (B) cryogenic temperatures, indicating that when the bath fluctuations are reduced and correlated at the two sites, charge separation involves the superposition of the two sites with renormalized coupling to the donor and the bath. The jagged lines represent the energy fluctuations over time of the acceptor sites resulting from interaction with the bath. Triplet states were omitted for clarity.

process was not observed. The loss of the RP relaxation process upon freezing the solvent suggests that the relaxation is associated with a relatively large amplitude structural modification, such as reorganization of the solvent shell or a change in the dihedral angle θ_d (Figure 1E). With no RP relaxation, the value of k_{CS} for **1** and **2** were determined by fitting kinetic traces at selected probe energies spanning the 3.28 eV ^{1*}**An** ESA to a single exponential decay convoluted with a Gaussian instrument response function using eq S2 (sample fits are presented in Figure S10 and Table S3). The resultant average rate constants are reported in Table 1. (see SI for fitting methodology). The ratio $[k_{CS}(\mathbf{2})/k_{CS}(\mathbf{1})] \pm \sigma$, where σ is the standard deviation, was determined to be 4.7 ± 0.8 (90 K, Figure 2F) and 5.0 ± 0.8 (5.5 K, Figure S11), where example kinetic traces for **1** and **2** are overlaid with simulated decay kinetics obtained from $2 \times k_{CS}(\mathbf{1})$ and $4 \times k_{CS}(\mathbf{1})$. The progressively lighter shading around the measured kinetic data illustrates up to 3σ of $\langle k_{CS} \rangle$. As another check, the same analysis performed on the room temperature data was also performed on the 90 K data, shown in Figure S9, to demonstrate that the two methods yield similar values for the rate enhancement. Thus, the data in Figures 2 and S9 show that $k_{CS}(\mathbf{2})$ is well-approximated by $4 \times k_{CS}(\mathbf{1})$, but not $2 \times k_{CS}(\mathbf{1})$, given the standard deviation of the experimental measurements.

The ratio $k_{CS}(\mathbf{2})/k_{CS}(\mathbf{1})$ observed at low temperatures (~5) shows a factor of two increase beyond that observed at room temperature (~2.4); see Figure 4. Changes in θ_d at low temperature are unlikely to be significant since the potential energy surface for rotation is broad, i.e. a large distribution of angles will be present in solution even at low temperatures.[26] Instead, we attribute the rate enhancement beyond the statistical limit to coherent interactions between the two acceptors and the bath, which can be either low-frequency solvent modes or internal modes of the sample.

The acceptor-acceptor and acceptor-bath interactions are summarized in Figure 3A-B for both room temperature and frozen solutions. Conventional ET theories such as the Marcus-Jortner treatment do not directly incorporate the effects of fluctuating system-bath interactions, let alone provide a framework for treating the effects of correlated fluctuations on ET. Instead, we implement the spin-boson model to treat the system-bath interactions explicitly, where k_{CS} can be expressed by eq 2, (see SI for details) assuming fast bath relaxation, weak system-bath coupling V_{SB}, and low temperature,[18,27-28]

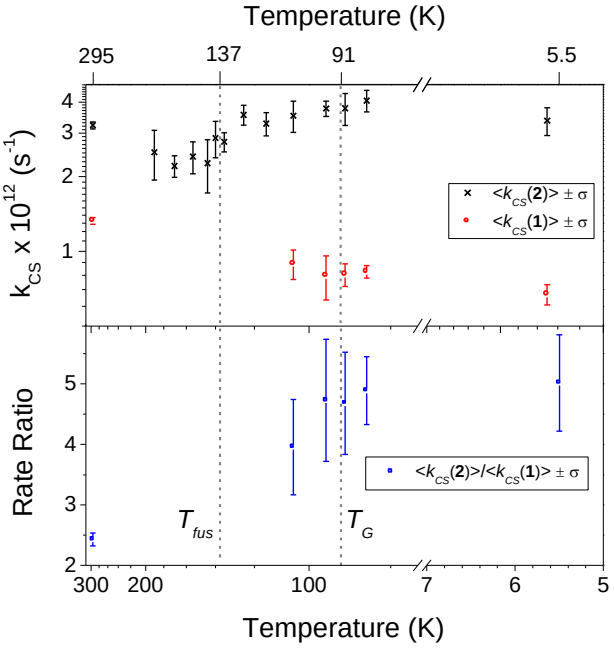

Figure 4. Average charge separation rate constants $\langle k_{CS} \rangle$ for **1** and **2** and ratio of rates at various temperatures between 295 and 5.5 K obtained from fitting kinetic traces at select probe energies with eq S2; error bars represent the standard deviation of the rate constant. Dashed gray lines represent the freezing point (T_{fus}) and glass transition temperature (T_G).

$$k_{CS} \propto \left(V_{DA}{}^2 V_{SB}^2\right)/(\Delta G_{CS})^2 \qquad (2)$$

as given by eq. 7.24 of Leggett, *et al.* [27] A brief derivation of this equation is also given in section III of reference 18 taking the low-temperature, large ΔG_{CS} limits. The free-energy dependence results from the donor-acceptor overlap integral, which diminishes with increasing ΔG_{CS}. At cryogenic temperatures, the fluctuations of the two **BQ**s and nearby solvent are decreased and the two acceptors (*RP* states) instead behave as two superposition states, a bonding state RP_+ and an antibonding state RP_- with normalized $V_{DA}(RP_+) = \sqrt{2}V_{DA}$ and $V_{DA}(RP_-) = 0$. In a similar manner, V_{SB} for the superposition bonding state RP_+ is renormalized to $\sqrt{2}V_{SB}$, as long as it originates from one or more modes that couple coherently to both **BQ**s, such that $k_{CS}(\mathbf{2}) \propto (\sqrt{2}V_{DA})^2(\sqrt{2}V_{SB})^2 = 4V_{DA}{}^2V_{SB}{}^2 = 4 \times k_{CS}(\mathbf{1})$. We note that this model is well-established theoretically[27] and accounts for both the increase and subsequent saturation of the value of $k_{CS}(\mathbf{2})/k_{CS}(\mathbf{1})$ over the broad low temperature range (100 - 5.5 K) as shown in Figure 4. The key result of this treatment is that the coherent interaction of the acceptor pair with the bath leads to an additional factor of 2 increase beyond the incoherent limit, consistent with our experimental observations of CS in frozen solution. Survival of the coherent dynamics, which here are likely correlated fluctuations of the energies or structures (e.g. in-phase vibrational motion) of the two **BQ**s, relies on the reduced random motion provided by the frozen solvent, similar to the proposed role of the protein matrix in protecting the chromophores from randomizing fluctuations in photosynthetic systems. Figure 4 shows the observed electron transfer rate constants for **1** and **2** as a function of temperature. The values of $k_{CS}(\mathbf{2})$ exhibit a sharp increase once the solution becomes supercooled and saturate near the glass transition temperature. In contrast, the

values for k_{CS}(**1**) exhibit no such increase. The different behavior in **1** and **2** further indicates a change in the CS mechanism in **2** from ET to a single **BQ** at higher temperatures to ET to a superposition of both **BQ**s at lower temperatures. Furthermore, the transition between incoherent (ET to a single **BQ**) and coherent (ET to a superposition of both **BQ**s) CS mechanisms occurs between the freezing and glassing temperatures, thus emphasizing the proposed role of solvent fluctuations in dictating which CS mechanism dominates.

These results highlight the importance of minimizing dephasing interactions in systems, such as OPV materials, where coherent interactions among donors and/or acceptors may provide crucial rate enhancements.

ASSOCIATED CONTENT

Supporting Information

Experimental details including instrumentation and synthesis, electrochemical and computational data, additional steady-state and transient optical data, and theoretical details.

AUTHOR INFORMATION

Corresponding Author

m-wasielewski@northwestern.edu
ryan.young@northwestern.edu

Present Addresses

BTP is currently at the Argonne National Laboratory, 9700 S. Cass Ave, Lemont, IL 60439, USA.
Y.-L W is currently at The School of Chemistry, Cardiff University, Main Building, Park Place, Cardiff, CF10 3AT, United Kingdom.

Author Contributions

‡These authors contributed equally.

Notes

The authors declare no competing financial interests.

ACKNOWLEDGMENT

We thank Dr. Aritra Mandal for helpful discussions and Jonathan Schultz for assistance with the temperature dependence measurements. This work was supported by the National Science Foundation under grant number DMR-1710104.

REFERENCES

(1) Cheng, Y.-C.; Fleming, G. R. *Annu. Rev. Phys. Chem.* **2009**, *60*, 241-262.

(2) Scholes, G. D.; Fleming, G. R.; Chen, L. X.; Aspuru-Guzik, A.; Buchleitner, A.; Coker, D. F.; Engel, G. S.; van Grondelle, R.; Ishizaki, A.; Jonas, D. M.; Lundeen, J. S.; McCusker, J. K.; Mukamel, S.; Ogilvie, J. P.; Olaya-Castro, A.; Ratner, M. A.; Spano, F. C.; Whaley, K. B.; Zhu, X. *Nature* **2017**, *543*, 647-656.

(3) Chenu, A.; Scholes, G. D. *Annu. Rev. Phys. Chem.* **2015**, *66*, 69-96.

(4) Duan, H.-G.; Prokhorenko, V. I.; Cogdell, R. J.; Ashraf, K.; Stevens, A. L.; Thorwart, M.; Miller, R. J. D. *Proc. Natl. Acad. Sci. U.S.A.* **2017**, *114*, 8493-8498.

(5) Niedringhaus, A.; Policht, V. R.; Sechrist, R.; Konar, A.; Laible, P. D.; Bocian, D. F.; Holten, D.; Kirmaier, C.; Ogilvie, J. P. *Proc. Natl. Acad. Sci. U. S. A.* **2018**, *115*, 3563-3568.

(6) Lee, H.; Cheng, Y.-C.; Fleming, G. R. *Science* **2007**, *316*, 1462-1465.

(7) Mohseni, M.; Rebentrost, P.; Lloyd, S.; Aspuru-Guzik, A. *J. Chem. Phys.* **2008**, *129*, 174106.

(8) Panitchayangkoon, G.; Hayes, D.; Fransted, K. A.; Caram, J. R.; Harel, E.; Wen, J.; Blankenship, R. E.; Engel, G. S. *Proc. Natl. Acad. sci. U.S.A.* **2010**, *107*, 12766.

(9) Collini, E.; Scholes, G. D. *Science* **2009**, *323*, 369-373.

(10) Bakulin, A. A.; Rao, A.; Pavelyev, V. G.; van Loosdrecht, P. H. M.; Pshenichnikov, M. S.; Niedzialek, D.; Cornil, J.; Beljonne, D.; Friend, R. H. *Science* **2012**, *335*, 1340-1344.

(11) Yu, J.; Zheng, Y.; Huang, J. *Polymers* **2014**, *6*, 2473-2509.

(12) Falke, S. M.; Rozzi, C. A.; Brida, D.; Maiuri, M.; Amato, M.; Sommer, E.; De Sio, A.; Rubio, A.; Cerullo, G.; Molinari, E.; Lienau, C. *Science* **2014**, *344*, 1001-1005.

(13) Marcus, R. A. *J. Chem. Phys.* **1965**, *43*, 679-701.

(14) Jortner, J. *J. Chem. Phys.* **1976**, *64*, 4860-4867.

(15) Skourtis, S. S.; Waldeck, D. H.; Beratan, D. N. *Annu. Rev. Phys. Chem.* **2010**, *61*, 461-485.

(16) Goldsmith, R. H.; Wasielewski, M. R.; Ratner, M. A. *J. Am. Chem. Soc.* **2007**, *129*, 13066-13071.

(17) Skourtis, S. S.; Waldeck, D. H.; Beratan, D. N. *J. Phys. Chem. B* **2004**, *108*, 15511-15518.

(18) Zarea, M.; Ratner, M. A.; Wasielewski, M. R. *J. Chem. Phys.* **2014**, *140*, 024110.

(19) Jansen, G.; Kahlert, B.; Klärner, F.-G.; Boese, R.; Bläser, D. *J. Am. Chem. Soc.* **2010**, *132*, 8581-8592.

(20) Jurczok, M.; Plaza, P.; Martin, M. M.; Meyer, Y. H.; Rettig, W. *Chem. Phys.* **2000**, *253*, 339-349.

(21) Shida, T. *Electronic Absorption Spectra of Radical Ions*; Elsevier: New York, 1988.

(22) Shida, T.; Iwata, S. *J. Am. Chem. Soc.* **1973**, *95*, 3473-3483.

(23) Lin, J.; Balamurugan, D.; Zhang, P.; Skourtis, S. S.; Beratan, D. N. *J. Phys. Chem. B* **2015**, *119*, 7589-7597.

(24) Ratner, M. A. *J. Phys. Chem.* **1990**, *94*, 4877–4883.

(25) Beratan, D. N.; Hopfield, J. J. *J. Am. Chem. Soc.* **1984**, *106*, 1584-1594.

(26) Sakata, K.; Hara, K. *Chem. Phys. Lett.* **2003**, *371*, 164-171.

(27) Leggett, A. J.; Chakravarty, S.; Dorsey, A. T.; Fisher, M. P. A.; Garg, A.; Zwerger, W. *Rev. Mod. Phys.* **1987**, *59*, 1-85.

(28) Nitzan, A. *Chemical dynamics in condensed phases: relaxation, transfer, and reactions in condensed molecular systems*; Oxford University Press: New York, USA, 2006.

Authors are required to submit a graphic entry for the Table of Contents (TOC) that, in conjunction with the manuscript title, should give the reader a representative idea of one of the following: A key structure, reaction, equation, concept, or theorem, etc., that is discussed in the manuscript. Consult the journal's Instructions for Authors for TOC graphic specifications.

TOC Graphic